Possible Evidence for Helical Nuclear Spin Order in GaAs Quantum Wires

C. P. Scheller,[1] T.-M. Liu,[1] G. Barak,[2] A. Yacoby,[2] L. N. Pfeiffer,[3] K. W. West,[3] and D. M. Zumbühl[1,*]
[1]Department of Physics, University of Basel, Klingelbergstrasse 82, CH-4056 Basel, Switzerland
[2]Department of Physics, Harvard University, Cambridge, Massachusetts 02138, USA
[3]Department of Electrical Engineering, Princeton University, Princeton, New Jersey 08544, USA
(Received 8 June 2013; published 10 February 2014)

We present transport measurements of cleaved edge overgrowth GaAs quantum wires. The conductance of the first mode reaches $2e^2/h$ at high temperatures $T \gtrsim 10$ K, as expected. As T is lowered, the conductance is gradually reduced to $1e^2/h$, becoming T independent at $T \lesssim 0.1$ K, while the device cools far below 0.1 K. This behavior is seen in several wires, is independent of density, and not altered by moderate magnetic fields B. The conductance reduction by a factor of 2 suggests lifting of the electron spin degeneracy in the absence of B. Our results are consistent with theoretical predictions for helical nuclear magnetism in the Luttinger liquid regime.

DOI: 10.1103/PhysRevLett.112.066801 PACS numbers: 73.21.Hb, 71.10.Pm, 73.23.Ad, 73.63.Nm

Conductance quantization is a hallmark effect of ballistic one-dimensional (1D) noninteracting electrons [1–4]. One mode of conductance e^2/h opens for each spin, giving conductance steps of $2e^2/h$ for spin degenerate electrons. In the presence of electron-electron (e-e) interactions, strongly correlated electron behavior arises, described by Luttinger liquid (LL) theory [5–7]. Salient LL signatures include ubiquitous power-law scaling [8–12], separation of spin and charge modes, and charge fractionalization—all recently observed [13–16] in cleaved edge overgrowth (CEO) GaAs quantum wires [17,18], thus establishing CEO wires as a leading realization of a LL. Interestingly, the conductance of a clean 1D channel is not affected by interactions, since it is given by the contact resistance in the Fermi liquid leads [19–23]. In the presence of disorder, however, the conductance is reduced with LL power laws [24,25]. While short constrictions display universal quantization [2,3], the ballistic CEO wires exhibit steps reduced below $2e^2/h$ at temperatures $T \geq 0.3$ K [26,27], presenting an unresolved mystery [11,13,26,28].

In this Letter, we revisit the conductance quantization in CEO wires, investigating for the first time low temperatures down to $T \sim 10$ mK. We find that the conductance of the first wire mode drops to $1e^2/h$ at $T \sim 100$ mK and remains fixed at this value for lower T, while the electron temperature cools far below 100 mK. At high $T \gtrsim 10$ K, the conductance approaches the expected universal value $2e^2/h$ [26]. This behavior suggests a lifting of the electron spin degeneracy at low T, in the absence of an external magnetic field B. The observed quantization values are quite robust, appearing in several devices, unaffected by moderate magnetic fields, and independent of the overall carrier density. A recent theory [29–31] predicts a drop of the conductance by a factor of 2 in the presence of a nuclear spin helix—a novel quantum state of matter. Our data agree well with this model, while other available theories are inconsistent with the experiments, thus offering a resolution of the nonuniversal conductance quantization mystery.

Ultraclean GaAs CEO double wires (DWs) were measured (inset, Fig. 1), similar to Refs. [13–16], offering mean free paths $\sim 20\ \mu$m and subband spacings exceeding 10 meV. Details on sample fabrication are given in [13,17,18,26,27]. A surface gate allows depletion of the 2D electron gas (2DEG) below, giving edge conduction in the DW only, forming what we will refer to as the "wire." Semi-infinite DWs with a few modes forming a 1D electron gas (1DEG) extend the wire on both sides, contacting the adjacent 2DEGs. Contacts to the 2DEGs are used to

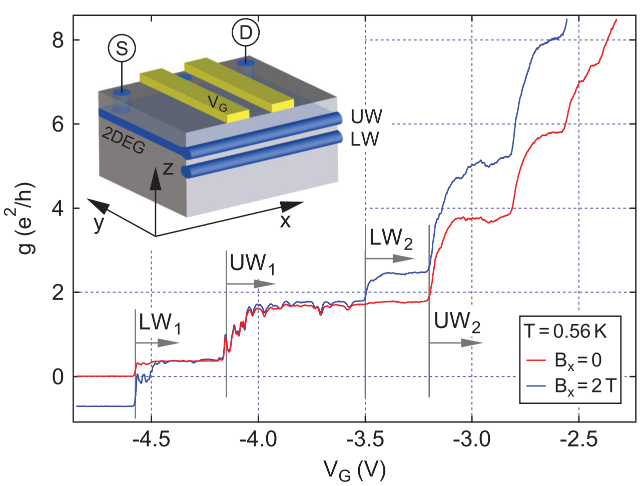

FIG. 1 (color). Double-wire mode structure. Differential conductance g (red) versus gate voltage V_G at $T = 0.56$ K and $B = 0$. Arrows indicate V_G above which modes start to contribute to g, as labeled. Blue data are at $B_X = 2$ T along the wire, offset in g to align LW_1 plateaus. The inset shows a sample schematic with a coordinate system.

measure the two-terminal differential conductance g of the wire.

The sample comprises an array of gates with 2 μm ungated spacing between 2 μm long wires, allowing individual and serial operation. In the ungated regions, the upper wire (UW) modes run directly adjacent to the 2DEG, resulting in a 2D-1D coupling length $\ell_{\text{2D-1D}} \sim 6$ μm [28]. The 1DEG to few-mode wire transition occurs on a length scale of about 500 nm—the distance of the UW and 2DEG to the surface gate—clearly longer than the Fermi wavelength $\lambda_F \lesssim 200$ nm, and, hence, in the adiabatic regime. The lower wire (LW), on the other hand, has no adjacent 2DEG and is only weakly tunnel coupled to the UW and 2DEG through a 6 nm thick AlGaAs barrier. UW to LW tunneling is very small in the gated segments. Thus, the 2 μm long DWs are considered as independent parallel resistors, with total conductance given by the sum of each conductance.

Figure 1 allows identifying the wire modes as a function of gate voltage V_G: increasing V_G starting from $g = 0$ at the most negative voltages, g is increasing in a steplike manner as the DW modes are populated one by one, as indicated. LW_n (UW_n) denotes the nth mode in the lower (upper) wire. Since the first step is small $\ll 2e^2/h$, it is associated with the tunnel coupled LW_1. The next, larger step corresponds to UW_1, followed by the LW_2 step, which becomes visible with a magnetic field $B_X = 2$ T along the wires (blue trace, shifted to align LW_1 plateaus). The tunneling process into the LW depends sensitively on parameters such as B, affecting the LW conductance. The next step has a large amplitude again and therefore corresponds to UW_2. Identifying higher modes is not easy due to a rapidly decreasing subband spacing.

The temperature dependence is shown in Fig. 2. At high T, the UW_1 step height is approaching $2e^2/h$, as expected for a spin degenerate single mode wire. The thermally excited subband population and resulting inclined plateaus start to become visible at high T, as well as a feature reminiscent of the 0.7 structure [32] at the low end of the plateau. At low T, on the other hand, the UW_1 conductance plateau is reduced strongly to $\sim 1e^2/h$, contrary to the 0.7 feature, which rises to $2e^2/h$ at low T [32]. In addition, the plateau develops pronounced, fully repeatable conductance oscillations. The same effect (transition from $g = 2e^2/h$ to $1e^2/h$) was seen in all four DWs, and also in single wires [see upper inset, Fig. 2(a)]. Because of the lower quality of the single wires currently available (note the short plateaus), measurements were largely done on DWs. CEO wires are extremely difficult to fabricate, limiting experiments to the present samples.

The oscillation pattern on the UW_1 plateau—complicating extraction of the step height—is reproduced independent of the number of modes transmitted through an adjacent wire. This indicates ballistic addition of quantized mode steps, as expected for a mean free path far exceeding

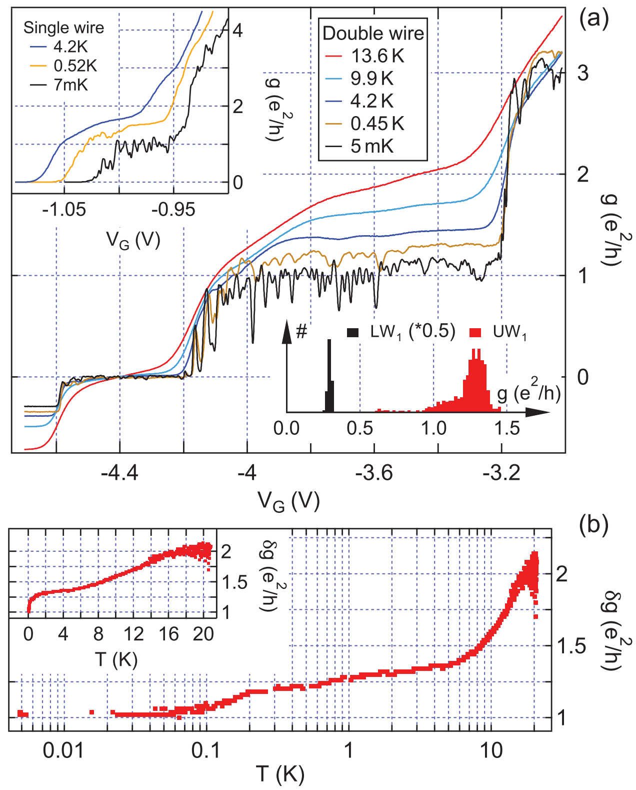

FIG. 2 (color). Temperature effects exhibiting conductance reduction by a factor of 2. (a) Gate voltage traces $g(V_G)$ at T as labeled, shifted in g to align LW_1 plateaus at $g = 0$. Similar measurements for a single wire are given in the upper inset. Lower inset: histogram of $g(V_G)$ for LW_1 and UW_1 regions (base temperature). (b) Conductance step height δg of UW_1 mode as a function of temperature on a logarithmic T axis (linear axis in inset), extracted from histogram peak positions (see main text). Small but discrete steps in g result from histogram binning.

the wire length. The oscillations are well understood as quantum interference caused by the finite size of the wire [33], giving maximal transmission ~ 1 at the conductance maxima. Indeed, the maxima of the oscillations neatly line up forming an upper ceiling on the UW_1 plateau, at intermediate T even forming flat tops; see Fig. 1. The minima, on the other hand, are rather dispersed over a range of conductances. A histogram extending over the first two conductance plateaus clearly reflects this behavior; see lower inset of Fig. 2(a). A long, asymmetric tail to low g on the UW_1 plateau (red) is seen below the peak at higher g. Therefore, we extract the peak positions $g_{\max \text{UW}_1}$ and $g_{\max \text{LW}_1}$ from the histogram and obtain the UW_1 conductance step height $\delta g = g_{\max \text{UW}_1} - g_{\max \text{LW}_1}$.

The temperature dependence of δg at $B = 0$ is displayed in Fig. 2(b) from 20 K down to 5 mK. Starting from the highest T, where δg reaches $2e^2/h$, lowering T continuously and monotonically decreases δg down to $\sim 1e^2/h$. We note that breaking of spin degeneracy would result in a reduction of the conductance by a factor of 2. At low

$T \lesssim 100$ mK, δg becomes temperature independent. However, the sample temperature cools far below 100 mK: first, thermal activation of fractional quantum Hall states can be used to extract an electron temperature ≤ 27 mK, clearly smaller than 100 mK. Note that this T is an upper bound only, since disorder can lead to deviation from exponential activation at low T. Occasional formation of a wire quantum dot [11] leads to lifetime broadened peaks not suitable for thermometry. Second, metallic Coulomb blockade thermometers [34] were measured under identical conditions, giving an electron temperature of 10.5 ± 0.5 mK at refrigerator temperature $T = 5$ mK. Details on filtering and heat sinking will be given elsewhere [35].

Next, we investigate the dependence on source-drain bias V_{SD}. Figures 3(a) and (b) show the conductance $g_{UW}(V_{SD})$ for V_G fixed on the UW_1 plateau. $g_{LW} \sim 0.3e^2/h$ depends only weakly on V_{SD}. At large $V_{SD} > 1$ mV, conductances around $2e^2/h$ are approached, while at low $V_{SD} \sim 0$, a sharp zero-bias anomaly (ZBA) of reduced $g_{UW} \lesssim 1e^2/h$ develops. While the ZBA could be related to the energy to destroy the nuclear spin helix, it could also have various other origins. Further, large bias causes resistive heating, raising temperature. Indeed, the $|V_{SD}|$ behavior and T dependence shown in Fig. 2(b) appear qualitatively very similar. Given the sharp ZBA, great care was taken to keep V_{SD} small throughout all linear response measurements ($V_{SD} = 3.5\ \mu$V, experimentally chosen to avoid nonlinear effects).

We now turn to the influence of a magnetic field. Figure 3(c) compares g at $B = 0$ and $B_Z = 2.8$ T

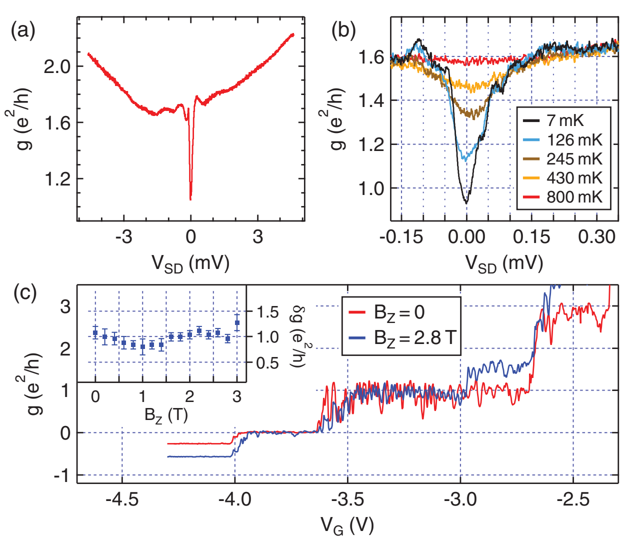

FIG. 3 (color). Bias and B-field dependence. (a),(b) g as a function of dc bias V_{SD}, for fixed V_G on the UW_1 plateau. (b) Different temperatures as labeled. (c) g at $B = 0$ (red) and $B_Z = 2.8$ T applied perpendicular to the 2DEG (blue), shifted in g to align the LW_1 plateau. The inset shows the conductance step height δg versus B_Z.

perpendicular to the 2DEG, at base T. While g_{LW} is changed, the step height δg is hardly affected at all: $\delta g(B_Z)$ remains close to $1e^2/h$ within the error bars [see inset Fig. 3(c)], despite Landau levels and edge states induced by B_Z in the 2DEG, reaching filling factor $\nu = 3$ at $B_Z = 3$ T. Further, the transitions from LW_1 to UW_1 at the larger B are comparable to $B = 0$ data (see, e.g., Fig. 4) and do not provide evidence for an additional plateau. Note that at 3 T, the Zeeman splitting is much larger than temperature, and the Landau level spin splitting is already resolved for much lower $B_Z \sim 0.3$ T. Finally, δg shows very little dependence on B_X (Fig. 1). Overall, we did not find evidence for qualitative changes of the UW_1 conductance step in moderate B fields.

We emphasize that the experiments [26,28], which studied single wires at $T \geq 300$ mK, are consistent with the results presented in this Letter. New here is the full g reduction to $g \sim 1e^2/h$, T independent for $T \lesssim 100$ mK, combined with the sharp zero-bias dip, B-field independence, and pronounced low-T conductance oscillations. In light of our new and complementary data, we now proceed to analyze different theories attempting to explain our findings, including reexamining models already discussed in Refs. [26,28]. First, noninteracting theories must be rejected: reduced conductance quantization within the Landauer formula results from nonideal transmission $t < 1$ [4], in contradiction to the observation of ballistic transport in our wires, in addition to the objections already raised in Ref. [26]. Our measurements with two wires in series show that t is at most a few percent below $t = 1$, in any case ruling out a g reduction by a factor of 2.

Second, we examine e-e interactions in the wire. A weakly disordered LL connected to Fermi liquid (FL) leads [25] gives conductances decreasing below $2e^2/h$ with a power law in V_{SD} and T. A finite conductance $\propto L^{-1}$ is obtained at $T = 0$ due to thermal freeze-out: when the thermal length L_T exceeds the wire length L at low enough T, g becomes T independent. However, here, $\delta g(T)$ remains clearly T dependent well below the freeze-out temperature $\sim$0.6 K (see Fig. 2) and further cannot reasonably be fit with a single power law over the entire T range. Therefore, LL theory for the 2 μm wire alone is an unlikely explanation.

Next, we consider e-e interactions also outside the wire. The 1DEGs may also experience non-FL correlations, albeit weaker than the wire since the 1DEGs are not single mode. The 2D-1D coupling scale $\ell_{2D-1D} \sim 6\ \mu$m sets an effective LL system length $L_{1DEG} = 2\ell_{2D-1D} + L$ comprised of segments ℓ_{2D-1D} on each side of the $L = 2\ \mu$m wire. As T is reduced, L_T first grows larger than L before eventually surpassing L_{1DEG}, where $g(T \to 0)$ saturates at $g_{sat} \propto 1/L_{1DEG}$. Hence, two temperature ranges with distinct power laws emerge, before g saturation at low T.

$\delta g(T)$ is consistent with such a model, giving decent agreement with two separate power-law fits. Further, a reasonable saturation temperature results: $L_T > L_{1\mathrm{DEG}}$ occurs on a temperature scale of ~0.1 K, where indeed the δg data is seen to lose T dependence. The value $g_{\mathrm{sat}} \sim 1e^2/h$ could then simply be a coincidence, but would depend on the details of the 2D-1D coupling. This coupling must involve scattering at an impurity or defect due to the large momentum mismatch between 1DEG and 2DEG electrons [26], and hence, within this model, g_{sat} will depend on parameters [36] such as disorder, chemical potential (density), and B fields.

Figure 4 displays $g(V_G)$ for a sequence of LED illumination [13] steps, ionizing more and more donors and thereby globally increasing the carrier density and mobility after each flash. The depletion voltage is proportional to density, and is seen to become more negative with increasing LED exposure, enhancing the density by over a factor of 2; see Fig. 4. Similarly, the 2D density and mobility increase by roughly a factor of 2 [before illumination, the density is 1×10^{11} cm^{-2} and the mobility $\sim 3 \times 10^6$ cm^2/(V s)]. Despite the large density change, the UW_1 step height (ceiling of the g oscillations) is seen to remain very close to $1e^2/h$. This is seen also in the other wires. In the absence of any significant density, disorder, wire, and B field dependence (see Figs. 1 and 3) of g_{sat}, this scenario has to be abandoned.

A further model put forth in [26] and refined in [28] proposed a competition between $\ell_{\mathrm{2D-1D}}$ and residual backscattering in the wires on a length $\ell_{\mathrm{BS}} \gg L$ for the reduced g plateaus. This model is expected to exhibit a similar sensitivity to the 2D-1D coupling details as above, and can again be ruled out based on the observations in Fig. 4, augmenting objections already raised in [26,28]. In addition, both $\ell_{\mathrm{2D-1D}}$ and ℓ_{BS} have (weak) LL power-law T dependence [37], leading to $g \to 0$ for $T \to 0$, in contradiction to the finite g_{sat} observed. Another scenario is an incoherent LL due to Wigner crystal formation [38,39]. In this model, g increases from $1e^2/h$ to $2e^2/h$ upon decreasing temperature, opposite to observations here. Further, very low densities $(a_B n)^{-1} \gg 1$ are required (a_B is the GaAs Bohr radius), which is not the case for the wires used here. Finally, spin orbit coupling has to be ruled out as well,

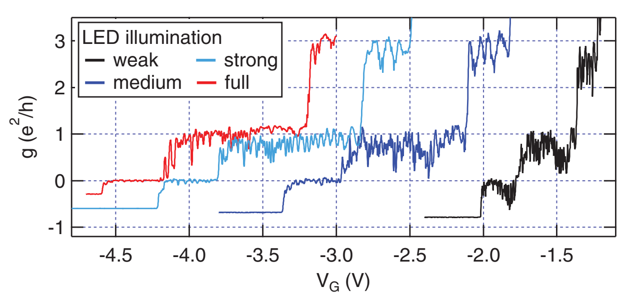

FIG. 4 (color). Density dependence $g(V_G)$ for a DW, recorded after LED illumination as labeled. Traces were shifted in g only to align the LW_1 plateau at $g = 0$. δg appears independent of flash strength and, hence, carrier density.

since the g reduction is seen at $B = 0$ and shows little B dependence.

A recent theory by Braunecker, Simon, and Loss [29–31] predicts helical nuclear spin order in a LL, causing a reduction of g by a factor of 2, from $2e^2/h$ to $1e^2/h$ for a clean wire, as seen in the experiment here. Below a crossover temperature T^*, an effective RKKY interaction, strongly enhanced by e-e interactions, forces the nuclear spin system via hyperfine interaction into helical order, constituting a novel state of matter. The resulting large Overhauser field acts back on the electronic system where a large gap opens—pinned at the Fermi energy—for half of the low energy modes, forming a helical LL and causing the g reduction at $B = 0$, applicable similarly for single and double wires [40]. The wire then only transmits spin-down right and spin-up left movers, therefore acting as a perfect spin filter. Note that the nuclear spin helix is a thermodynamic ground state protected by a gap, rather than a dynamic nuclear spin polarization.

The predicted T^* depends very strongly on the charge LL parameter K_C and can exceed 1 K for small K_C (strongly interacting) [29]. Full nuclear order is obtained only at $T \ll T^*$ and zero polarization only at $T \gg T^*$. Estimating K_C is far from trivial both experimentally and theoretically [14]: $K_C = 0.4$ gives $T^* \sim 0.2$ K and $K_C = 0.3$ already $T^* \sim 0.6$ K, consistent with the experiment. Further, large T^* result in a rather broad, washed-out transition, as observed in the experimental $\delta g(T)$. K_C is expected to depend (weakly) on density n, therefore T^* will change over a conductance plateau. However, given a very broad transition, this may affect g only weakly, and give rather flat conductance plateaus, as seen in the experiment. Further, the theory derives g far below and above, rather than throughout, the nuclear transition, allowing only a qualitative comparison. Finally, a Zeeman splitting much smaller than the induced gap should affect neither the nuclear order nor the conductance, as seen in the experiment.

In summary, we have investigated conductance quantization in single mode LL wires, finding a very broad transition at $B = 0$ from $2e^2/h$ at high T to $1e^2/h$ at low $T \lesssim 100$ mK, where g becomes T independent. This behavior is consistently seen in double and single wires, is independent of overall density and disorder (2D-1D coupling, illumination), is destroyed with bias V_{SD} similar to T, and is insensitive to moderate B fields. All these observations are in good agreement with a nuclear spin helix model [29–31], which predicts a crossover temperature T^* in the observed range, while all other theories considered here and previously [26,28] are inconsistent with the data. While we cannot rule out other explanations we are not aware of, we emphasize that the data are striking and stand alone, irrespective of the model used for interpretation.

Further experiments are needed to investigate the role of the nuclear spins. Resistively detected NMR was already attempted here: while detecting clear 2DEG signals, no identifiable NMR response was found for the wires. However, it is difficult to estimate what the effect of an NMR excitation is, what the low energy nuclear spin excitations are, and whether a detectable resistive signal would result. Spectroscopic methods [13] might be used to shed more light on the electronic structure. In the nuclear spin helix state, the electron system is in the helical LL regime, equivalent to a spin-selective Peierls transition in a Rashba spin-orbit coupling wire [30]. Given proximity to an *s*-wave superconductor, a topological phase sustaining Majorana fermions could be created.

We would like to thank O. Auslaender, B. Braunecker, D. Loss, D. L. Maslov, T. Meng, M. Meschke, J. Pekola, P. Simon, and Y. Tserkovnyak for valuable input and stimulating discussions. This work was supported by the Swiss Nanoscience Institute (SNI), NCCR QSIT, Swiss NSF, ERC starting grant, and EU-FP7 SOLID and MICROKELVIN. A. Y. acknowledges support from the NSF DMR-1206016. The work at Princeton was partially funded by the Gordon and Betty Moore Foundation through Grant No. GBMF2719, and by the National Science Foundation MRSEC-DMR-0819860 at the Princeton Center for Complex Materials.

*dominik.zumbuhl@unibas.ch

[1] R. Landauer, IBM J. Res. Dev. **1**, 223 (1957).
[2] B. J. van Wees, H. van Houten, C. W. J. Beenakker, J. G. Williamson, L. P. Kouwenhoven, D. van der Marel, and C. T. Foxon, Phys. Rev. Lett. **60**, 848 (1988).
[3] D. A. Wharam, T. J. Thornton, R. Newbury, M. Pepper, H. Ahmed, J. E. F. Frost, D. G. Hasko, D. C. Peacock, D. A. Ritchie, and G. A. C. Jones, J. Phys. C **21**, L209 (1988).
[4] C. W. J. Beenakker and H. van Houten, in *Solid State Physics*, edited by H. Ehrenreich and D. Turnbull, Semiconductor Heterostructures and Nanostructures (Academic Press, New York, 1991).
[5] S.-I. Tomonaga, Prog. Theor. Phys. **5**, 544 (1950).
[6] J. M. Luttinger, J. Math. Phys. (N.Y.) **4**, 1154 (1963).
[7] F. D. M. Haldane, J. Phys. C **14**, 2585 (1981).
[8] A. M. Chang, L. N. Pfeiffer, and K. W. West, Phys. Rev. Lett. **77**, 2538 (1996).
[9] M. Bockrath, D. H. Cobden, J. Lu, A. G. Rinzler, R. E. Smalley, L. Balents, and P. E. McEuen, Nature (London) **397**, 598 (1999).
[10] H. W. C. Postma, T. Teepen, Z. Yao, M. Grifoni, and C. Dekker, Science **293**, 76 (2001).
[11] O. M. Auslaender, A. Yacoby, R. de Picciotto, K. W. Baldwin, L. N. Pfeiffer, and K. W. West, Phys. Rev. Lett. **84**, 1764 (2000).
[12] Y. Tserkovnyak, B. I. Halperin, O. M. Auslaender, and A. Yacoby, Phys. Rev. B **68**, 125312 (2003).
[13] O. M. Auslaender, A. Yacoby, R. de Picciotto, K. W. Baldwin, L. N. Pfeiffer, and K. W. West, Science **295**, 825 (2002).
[14] O. M. Auslaender, H. Steinberg, A. Yacoby, Y. Tserkovnyak, B. I. Halperin, K. W. Baldwin, L. N. Pfeiffer, and K. W. West, Science **308**, 88 (2005).
[15] H. Steinberg, G. Barak, A. Yacoby, L. N. Pfeiffer, K. W. West, B. I. Halperin, and K. L. Hur, Nat. Phys. **4**, 116 (2008).
[16] G. Barak, H. Steinberg, L. N. Pfeiffer, K. West, L. Glazman, F. Oppen, and A. Yacoby, Nat. Phys. **6**, 489 (2010).
[17] L. N. Pfeiffer, H. L. Stormer, K. W. Baldwin, K. W. West, A. R. Goi, A. Pinczuk, R. C. Ashoori, M. M. Dignam, and W. Wegscheider, J. Cryst. Growth **127**, 849 (1993).
[18] W. Wegscheider, W. Kang, L. N. Pfeiffer, K. W. West, H. L. Stormer, and K. W. Baldwin, Solid State Electron. **37**, 547 (1994).
[19] D. L. Maslov and M. Stone, Phys. Rev. B **52**, R5539 (1995).
[20] I. Safi and H. J. Schulz, Phys. Rev. B **52**, R17040 (1995).
[21] V. V. Ponomarenko, Phys. Rev. B **52**, R8666 (1995).
[22] Y. Oreg and A. M. Finkel'stein, Phys. Rev. B **54**, R14265 (1996).
[23] R. de Picciotto, H. L. Stormer, L. N. Pfeiffer, K. W. Baldwin, and K. W. West, Nature (London) **411**, 51 (2001).
[24] S. Tarucha, T. Honda, and T. Saku, Solid State Commun. **94**, 413 (1995).
[25] D. L. Maslov, Phys. Rev. B **52**, R14368 (1995).
[26] A. Yacoby, H. L. Stormer, N. S. Wingreen, L. N. Pfeiffer, K. W. Baldwin, and K. W. West, Phys. Rev. Lett. **77**, 4612 (1996).
[27] A. Yacoby, H. L. Stormer, K. W. Baldwin, L. N. Pfeiffer, and K. W. West, Solid State Commun. **101**, 77 (1997).
[28] R. de Picciotto, H. L. Stormer, A. Yacoby, L. N. Pfeiffer, K. W. Baldwin, and K. W. West, Phys. Rev. Lett. **85**, 1730 (2000).
[29] B. Braunecker, P. Simon, and D. Loss, Phys. Rev. B **80**, 165119 (2009).
[30] B. Braunecker, G. I. Japaridze, J. Klinovaja, and D. Loss, Phys. Rev. B **82**, 045127 (2010).
[31] B. Braunecker, P. Simon, and D. Loss, Phys. Rev. Lett. **102**, 116403 (2009).
[32] K. J. Thomas, J. T. Nicholls, M. Y. Simmons, M. Pepper, D. R. Mace, and D. A. Ritchie, Phys. Rev. Lett. **77**, 135 (1996).
[33] C. P. Scheller, T.-M. Liu, A. Yacoby, L. N. Pfeiffer, K. W. West, and D. M. Zumbühl (to be published).
[34] L. Casparis, M. Meschke, D. Maradan, A. C. Clark, C. P. Scheller, K. K. Schwarzwlder, J. P. Pekola, and D. M. Zumbühl, Rev. Sci. Instrum. **83**, 083903 (2012).
[35] C. P. Scheller, S. Heizmann, K. Bedner, M. Meschke, J. Pekola, and D. M. Zumbühl (to be published).
[36] Y. Tserkovnyak (private communication).
[37] $l_{2D-1D} \propto T^{-p_1}$ and $l_{BS} \propto T^{p_2}$, with $0 < p_{1,2} < 1$.
[38] K. A. Matveev, Phys. Rev. Lett. **92**, 106801 (2004).
[39] K. A. Matveev, Phys. Rev. B **70**, 245319 (2004).
[40] T. Meng and D. Loss, Phys. Rev. B **87**, 235427 (2013).